

Value of Magnetic Resonance Spectroscopy in Differentiation between Residual/Recurrent Primary Brain Tumors and Radiation Necrosis

Ahmed S. Abd-El-Fattah^a, Jehan I. Al-Tohamy^b, Mohammed E. Abd-Elsamea^c, Hesham E. El-Sheikh^a, Sherif A. Abd-Elsattar^a

^aDepartment of Diagnostic and Interventional Radiology, Faculty of Medicine; Benha University, Egypt.

^aDepartment of Diagnostic and Interventional Radiology, Armed forces college of medicine AFCEM and General organization for teaching hospitals and institutes GOTH.

^aDepartment of Diagnostic and Interventional Radiology, National Liver Institute - Menoufia University, Egypt.

Correspondence to:

Ahmed S. Abd-El-Fattah, Department of Diagnostic and Interventional Radiology, Faculty of Medicine; Benha University, Egypt.

Email:

ahmadazmy8893@gmail.com

Received:

Accepted

Abstract

Background: Residual/recurrent tumors are the primary clinical challenge encountered during the diagnostic workup of cases who have received prior treatment for brain tumors. Magnetic resonance spectroscopy was employed to assess the efficacy of this examination in recognizing radiation necrosis (RN) from residual/recurrent primary brain lesions.

Methods: This prospective study enrolled 30 patients with primary brain tumors receiving radiotherapy and under follow-up at the Radiology Department of Benha University hospitals. All patients were divided into 2 groups according to MRS diagnosis: Group I (n=7): patients with RN and group II (n=23): patients with recurrent tumors. **Results:** MRS diagnosis using Choline (Cho) / N-acetyl aspartate (NAA) had 72% sensitivity, 60% specificity, 90% Positive (PPV) and 30% Negative (NPV) predictive values and 70% diagnostic accuracy. MRS diagnosis using Cho/Creatine (Cr) had 85.71% sensitivity, 55.56% specificity, 81.82% PPV, 62.50% NPV and 76.67% diagnostic accuracy. The proposed final diagnosis had 84.21% sensitivity, 75.00% specificity, 84.21% PPV, 75.00% NPV and 83.33% diagnostic accuracy.

Conclusion: The differentiation between tumor recurrence and RN is facilitated by MRS, which is both safe and informative. Examination of numerous regions of the high-volume lesions is necessary. Recurrent malignancies were significantly more accurately predicted by the Cho/NAA and Cho/Cr ratios, as indicated by the meta-analysis. In this regard, MRS imaging functions as an informative instrument for the differentiation of necrosis and tumor recurrence.

Keywords: Magnetic Resonance Spectroscopy, Radiation Necrosis, Residual/Recurrent Primary Brain Tumors.

Introduction

During the diagnostic workup of patients who have undergone prior treatment for brain tumors, the identification of residual or recurrent tumors is the most significant clinical challenge ⁽¹⁾. Magnetic resonance imaging (MRI) and contrast-enhanced computed tomography (CT) are indispensable for contemporary brain tumor diagnostic evaluations ⁽²⁾. Brain tumors are most frequently caused by gliomas, which are derived from glial cells in the brain. Radiation therapy is one of the most effective adjuvant treatments for malignant central nervous system (CNS) malignancies in conjunction with surgery ⁽³⁾. Delayed neurological complications and deficits in long-term survivors are the primary complications of brain irradiation, which is caused by late radiation injury. Contralateral lesions are rarely reported, despite the fact that cerebral RN typically manifests at or near the primary lesion's location ^(4, 5).

The RN pattern that is most frequently observed is defined by a single lesion that appears at or near the original tumor site. The residual or recurrent tumor can be easily misidentified, and both can present as an enhancing mass that expands over time and exhibits the exertion of mass effects ⁽⁵⁾. During the post-radiation follow-up of cases with malignant gliomas, it is essential to distinguish between RN and tumor recurrence. MRI reveals contrast enhancement in recurrent neoplasms (RN) and recurrent tumors owing to the disruption of the blood-brain barrier. As a consequence, RN may be indistinguishable from tumor residue/recurrence based solely on

imaging. Results of MRI are relatively non-specific ⁽⁶⁾.

During MRI, stereotactic biopsy may be implemented to evaluate suspicious findings. Unfortunately, this procedure is linked to a risk of morbidity. Furthermore, approximately 10% of biopsy results are imprecise owing to sampling errors ⁽⁶⁾. Innovative MRI approaches, such as proton magnetic resonance spectroscopy (MRS), have the potential to offer a more precise identification of treatment-related alterations ⁽⁷⁾.

The metabolic composition of a specific tissue area can be further elucidated by contrasting the relative concentration of multiple metabolites using proton magnetic resonance spectroscopy (1H MRS). MRS ability to facilitate a more comprehensive assessment of indeterminate intracranial mass lesions is demonstrated by the provision of data on metabolic modifications, including those that are pertinent to cellular turnover or proliferative activity (choline), a reduction in neuronal density (N-acetyl-aspartate), and the presence of necrosis (lipids, lactate) ⁽⁸⁾.

This work aimed to determine the value of MRS in differentiation between residual/recurrent primary brain tumors and RN.

Patients and Methods

This prospective study enrolled 30 patients with primary brain tumors who received radiotherapy and under follow-up at the Radiology Department of Benha

University hospitals for 1 year from January 2024 to January 2025. All participants provided written informed consent. The study commenced following approval by the Ethics Committee of the Faculty of Medicine, Benha University (approval code: MD 1-3-2023).

Inclusion criteria: Patients of any age group and sex, patients with primary brain tumors receiving radiotherapy who were undergo MRS examination and patients approved to be included in the research with informed written consent.

Exclusion criteria: Patients lost to follow-up, patients with contraindication to IV contrast media administration, claustrophobia, metal implants as cochlear implants, cardiac defibrillators and pacemakers and patients who refused to take part in the research.

Grouping:

All patients were divided into 2 groups based on MRS diagnosis: Group I (n=7): patients with RN and group II (n=23): patients with recurrent tumors.

All patients underwent history taking including [demographics: (age, sex, medical history, surgical history, radiation therapy history and body mass index (BMI), presenting symptoms including (headache, seizures, focal neurological deficits, cognitive changes), onset and progression of symptoms, previous imaging studies including (MRI, CT, PET), treatment history including (surgery, chemotherapy, radiation therapy), physical examination including clinical examinations, heart rate, systolic and diastolic blood pressure, assessment of body weight, and BMI ^[9], Concurrently

with the assessment of vital signs, such as blood pressure, temperature, respiratory rate, and pulse rate, a neurological examination is conducted. This assessment encompasses the motor system, the sensory system, the cranial nerves, and reflexes. In addition, a comprehensive blood profile (hemoglobin, red blood cells, white blood cells, and platelet count), lipid profile (cholesterol, high density lipoprotein, low density lipoprotein, and triglycerides), liver function test (alanine transaminase and aspartate transferase), and kidney function test (creatinine and urea) are carried out. In addition, laboratory investigations are also implemented. The analysis of FLAIR, diffusion-weighted images (DWI), T1-weighted, T2-weighted, and MRS sequences is facilitated by MRI with MRS. Additionally, positron emission tomography (PET) and CT imaging are viable alternatives.

Case preparation including detailed explanation of the procedure to the case or case relatives according to their condition, following the acquisition of informed consent from the cases or their relatives, the case was subjected to a comprehensive history. MRS was performed during the conventional acquisition of MRI using the 1.5-T MR apparatus, Magnetom, Vision (Siemens, Erlangen, Germany). Single-voxel techniques were implemented for minor lesions, with a standard voxel volume of 8.0 cm³ (2.0 × 2.0 × 2.0 cm) or a minimum of 3.37 cm³ (1.5 × 1.5 × 1.5 cm). With a TE of 144 ms, the acquisition parameters were configured to employ the Press technique. Saturation was subsequently selected chemically to suppress water, and shimming was executed automatically. To the utmost

extent feasible, the cranium and cranial base were safeguarded from signal contamination by adipose tissue. Prior to the administration of gadolinium-diethylenetriamine penta-acetic acid (Gd-DTPA), the voxels were positioned on T2-weighted images of the lesions to acquire uniformly adjusted spectra. Subsequently, we employed Gd-DTPA to perform T1-weighted MR imaging to verify the spatial relationship between the spectroscopic voxel and the enhanced lesion. Nitrous oxide and halothane were administered to cases under the age of 10 to induce sedation in order to facilitate inert examinations. The y-axis used an arbitrary intensity scale to display the height of the metabolite peaks, while the x-axis consistently displayed metabolites in parts per million (ppm). N-acetyl aspartate (NAA) was measured at 2.01 ppm, lipid at 0.8-1.3 ppm, and choline (Cho) at 3.22 ppm in the metabolites under investigation.

Protocol of MRI

T1 weighted spin-echo images (Repetition Time (TR)=400-500ms, TE=15-20ms, Field-of-view (FOV) =200mm, acquisition matrix=256x141 pixels, slice thickness=4mm, with 0.5mm gap). T2 weighted spin-echo images (TR=3500-5000ms, TE=100-120ms, FOV=200mm, acquisition matrix=512x301 pixel, slice thickness=4mm, with 0.5mm gap). Axial FLAIR images (TR=11000ms, TE=140ms, inversion time=2800ms, FOV=200mm, acquisition matrix=256x137 pixels, slice thickness=4mm, with 0.5mm gap). Axial DWI (TR=3160ms, TE=100ms, FOV=200mm, acquisition matrix=256x77pixels, slice thickness=4mm, with 0.5mm gap). T1

weighted spin-echo images after the injection of Intravenous (IV) gadolinium (TR=400-500ms, TE=15-20ms, FOV=200mm, acquisition matrix=256x141 pixels, slice thickness=4mm, with 0.5mm gap). The dose of gadolinium injection is 0.1mmol/kg.

Acquisition of spectroscopic data

In two phases, the ¹H MRS programming was conducted using T2-weighted HASTE sequences. The initial stage utilized exclusively sagittal images at maximum inspiration and expiration, as well as free breathing. The multivoxel grid was meticulously positioned at the lesion's center, and all three sagittal sequences were employed to encompass the maximum amount of the lesion area or, preferably, the entire lesion and a portion of the adjacent tissue. Following the establishment of the field of view and shimming dimensions, the second phase of the programming was implemented, which involved the expiration of three orthogonal planes. This procedure was developed to ascertain the thickness of the voxel, enable the operation of only the radiofrequency coil that is adjacent to the mass or nodule, and position the external saturation bands. The ¹H MRS sequence offered the flexibility to employ six 30 mm-thick external saturation bands, which would mitigate the effects of the magnetic susceptibility non-homogenization of the field. Additionally, it allowed for the freedom to be angled in a variety of ways without compromising spectroscopic acquisition. Spectra were obtained from an 8cc single voxel in a normal-appearing white matter region of the left or right parietal hemisphere, which was

surrounded by a gadolinium (Gad) enhancing lesion or a non-enhancing hypointense T1 lesion.

Statistical analysis:

For the statistical research, I used SPSS v26, a program created and maintained by IBM in Armonk, NY, USA. To compare the two groups for quantitative characteristics, we used an unpaired Student's t-test. Both the means and the standard deviations (SD) of the data were presented. Qualitative variables were analyzed using Fisher's exact test or a chi-square test where appropriate. The variables were presented as percentages and frequencies, respectively. Statistical significance was determined by a two-tailed P value less than 0.05. Assessment of the accuracy of diagnostic tests administered: For diagnostic sensitivity, we look at the percentage of positive findings in case groups and for diagnostic specificity, we look at the percentage of negative results in healthy groups. The percent of genuine positive outcomes in relation to the total number of positive results is known as the positive predictive value (PPV). The NPV is the fraction of entirely negative outcomes that are really negative predictions.

Results

The mean of age of the total cases was 39.3 ± 13.84 years. There was 16 (53.33%) males and 14 (46.67%) females. The mean of weight of the total was 78.2 ± 10.98 Kg, the mean of height was 1.66 ± 0.04 m and the mean of BMI was 28.47 ± 4.69 Kg/m². Among the total cases, 9 (30%) cases had hypertension and 8 (26.67%) cases had diabetes mellitus. Regarding the primary

pathology, the majority of the studied cases 18 (60%) had glioblastoma, 4 (13.33%) cases had low-grade astrocytoma, 3 (10%) cases had anaplastic astrocytoma, 2 (6.67%) cases had oligodendroglioma, 2 (6.67%) cases had CNS lymphoma and only 1 (3.33%) case had medulloblastoma. (**Table 1**)

Pathological MR spectra indicative of recurrent/residual tumor demonstrated significantly increased Choline peak, markedly diminished NAA along with prominent lipid/lactate peaks, while the pathological spectra characteristic for radiation necrosis showed slightly increased choline peak, mildly reduced NAA peak and mild elevation of lipid/lactate peaks. (**Fig. 1, Fig. 2, Fig. 3, Fig. 4**)

(**Table 2**) showed that the mean of radiation dose was 39.3 ± 13.84 Gy. The interval between completion of radiotherapy to MRS diagnosis with a mean of 17.33 ± 8.6 months. Regarding the diagnosis of the studied cases, MRS diagnosis showed that recurrent tumors in 23 (76.67%) cases and RN in 7 (23.33%) cases. By histopathologic diagnosis, 24 (80%) cases had recurrent tumors and 6 (20%) cases had RN. Regarding the metabolic ratio of the total, the mean of Cho / NAA ratio was 2.56 ± 1.11 and the mean of Cho / Cr ratio was 2.79 ± 1.6 .

The mean interval between completion of radiotherapy to MRS diagnosis was insignificantly different between cases with RN and those with recurrent tumors. Cho/NAA and Cho/Cr were significantly elevated in cases with recurrent tumors compared to those with RN ($P=0.008$, <0.001). (**Table 3**)

MRS diagnosis using Cho/NAA had 72% sensitivity, 60% specificity, 90% PPV, 30% NPV and 70% diagnostic accuracy. MRS diagnosis using Cho/Cr had 85.71% sensitivity, 55.56% specificity, 81.82%

PPV, 62.50% NPV and 76.67% diagnostic accuracy. The proposed final diagnosis had 84.21% sensitivity, 75.00% specificity, 84.21% PPV, 75.00% NPV and 83.33% diagnostic accuracy. (**Table 4**)

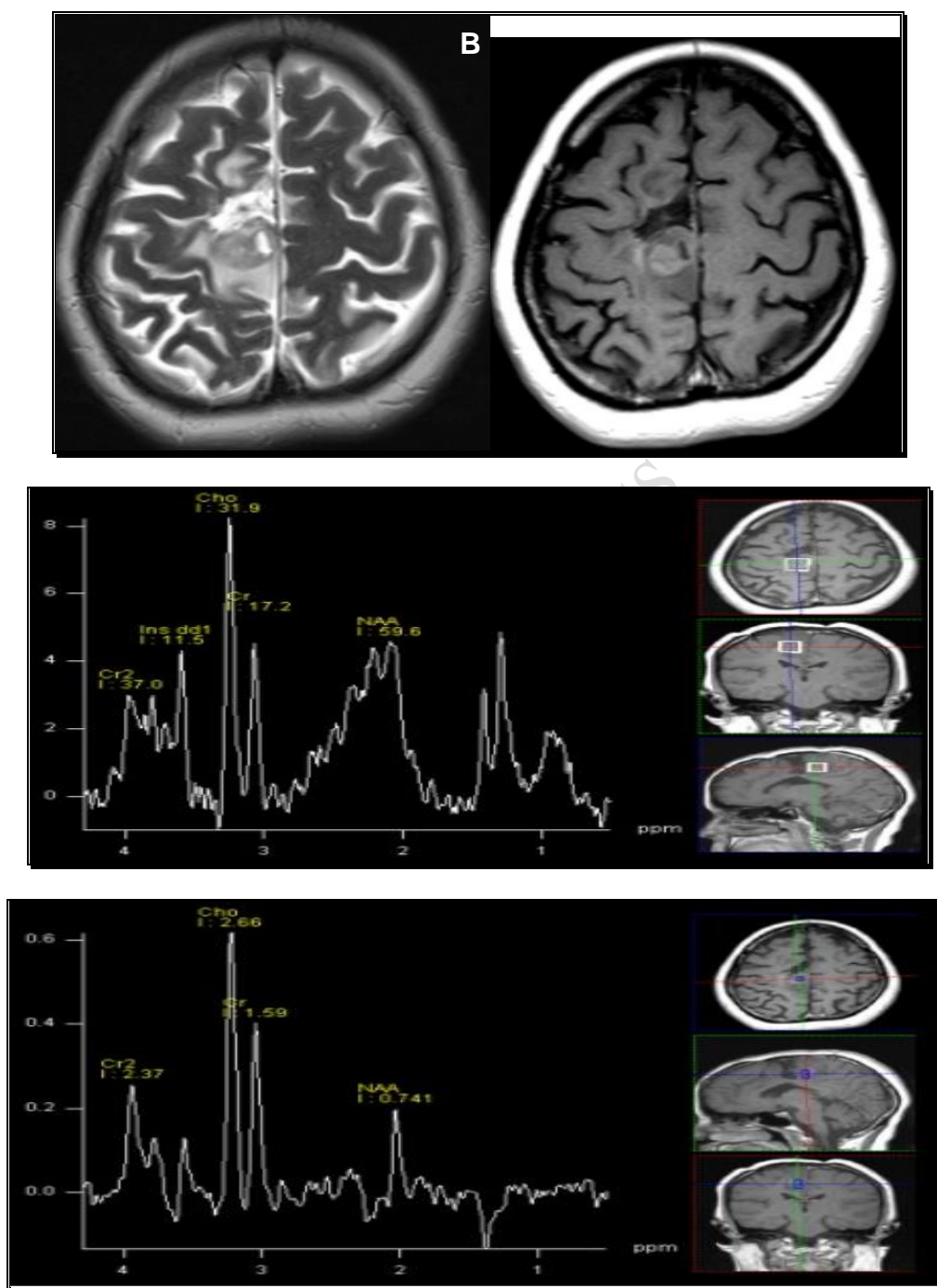


Figure (1): Recurrent tumor. Follow-up MRI and MRS study after receiving resection and radiotherapy for right cerebral grade IV glioblastoma. Axial T2 weighted image (**A**) showing right high frontal abnormal mixed hypointense and hyperintense signal with mild perilesional edema. Post-contrast axial T1 weighted image (**B**) showing small enhancing space occupying lesion. MRS with short (**C**) and long TE (**D**) with the volume placed over the enhancing lesion showing significantly elevated choline peak, with decreased NAA and Cr peaks, and prominent lipid and lactate peaks. There is elevated Cho/NAA ratio (3.56) and Cho/Cr ratio (3.2).

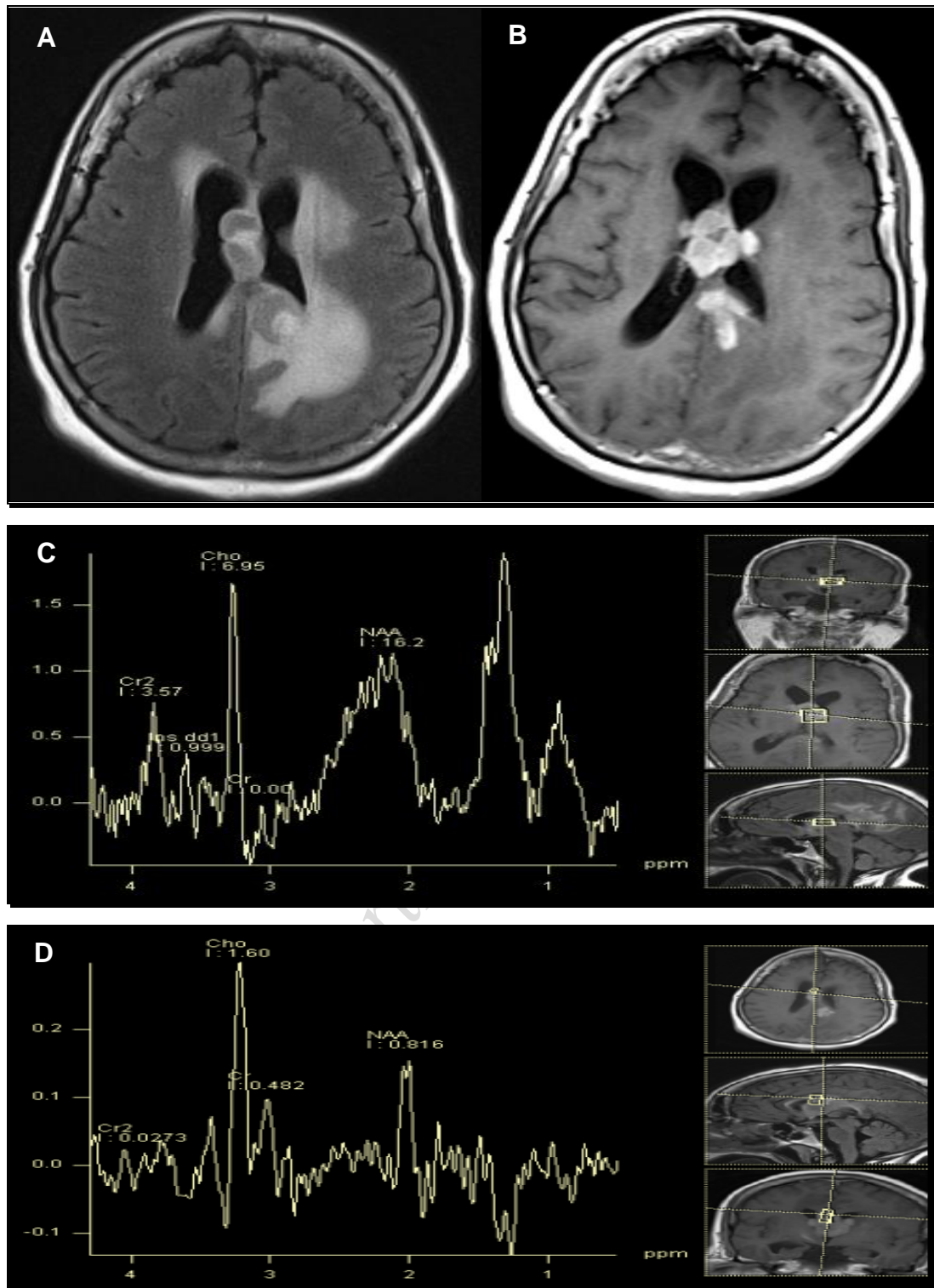


Figure (2): Residual tumor. Follow-up MRI and MRS study after receiving chemoradiotherapy for periventricular CNS lymphoma. Axial FLAIR (A) showing periventricular space occupying lesion involving the corpus callosum with surrounding vasogenic edema. Post-contrast axial T1 weighted image (B) showing intense enhancement of the lesion. MRS with short (C) and long TE (D) with the volume placed over the enhancing lesion showing significantly elevated choline peak, with decreased NAA and Cr peaks, and prominent lactate peak. There is elevated Cho/NAA ratio (2.12) and Cho/Cr ratio (2.9).

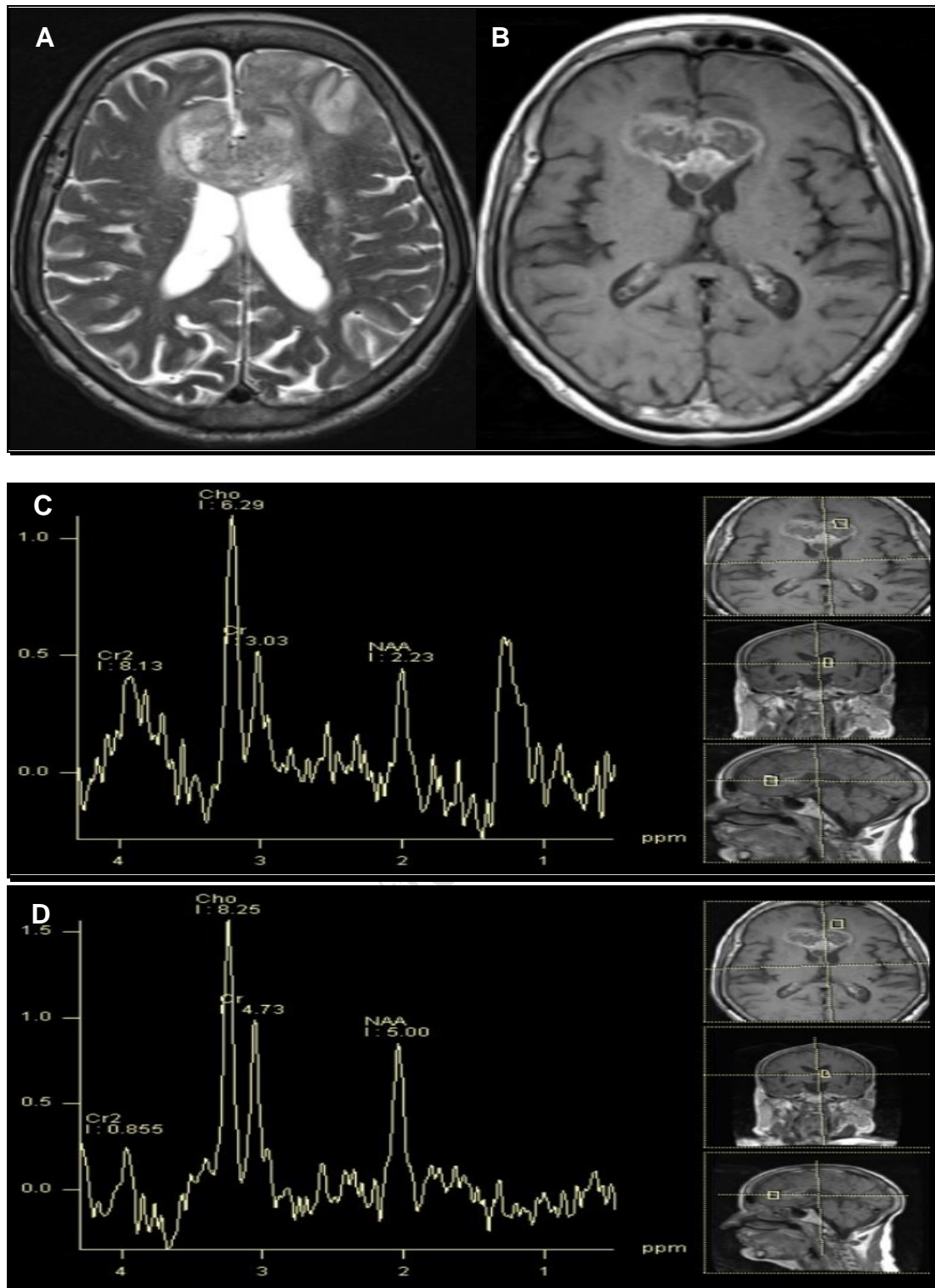


Figure (3): Residual tumor. Follow-up MRI and MRS study after receiving chemoradiotherapy for grade IV glioblastoma. Axial T2 weighted image (A) showing heterogeneous signal crossing corpus callosum into both frontal lobes. Post-contrast axial T1 weighted image (B) showing avid peripheral contrast enhancement of the space occupying lesion. MRS with short TE (C) showing significantly elevated choline peak, with decreased NAA and Cr peaks, and prominent Lipid/lactate peak. There is elevated Cho/NAA ratio (3.79) and Cho/Cr ratio (3.1). Perilesional voxel with long TE (D) showing substantial elevation of choline peak, with Cho/NAA ratio (2.76) and Cho/Cr ratio (1.9), indicating perilesional infiltration.

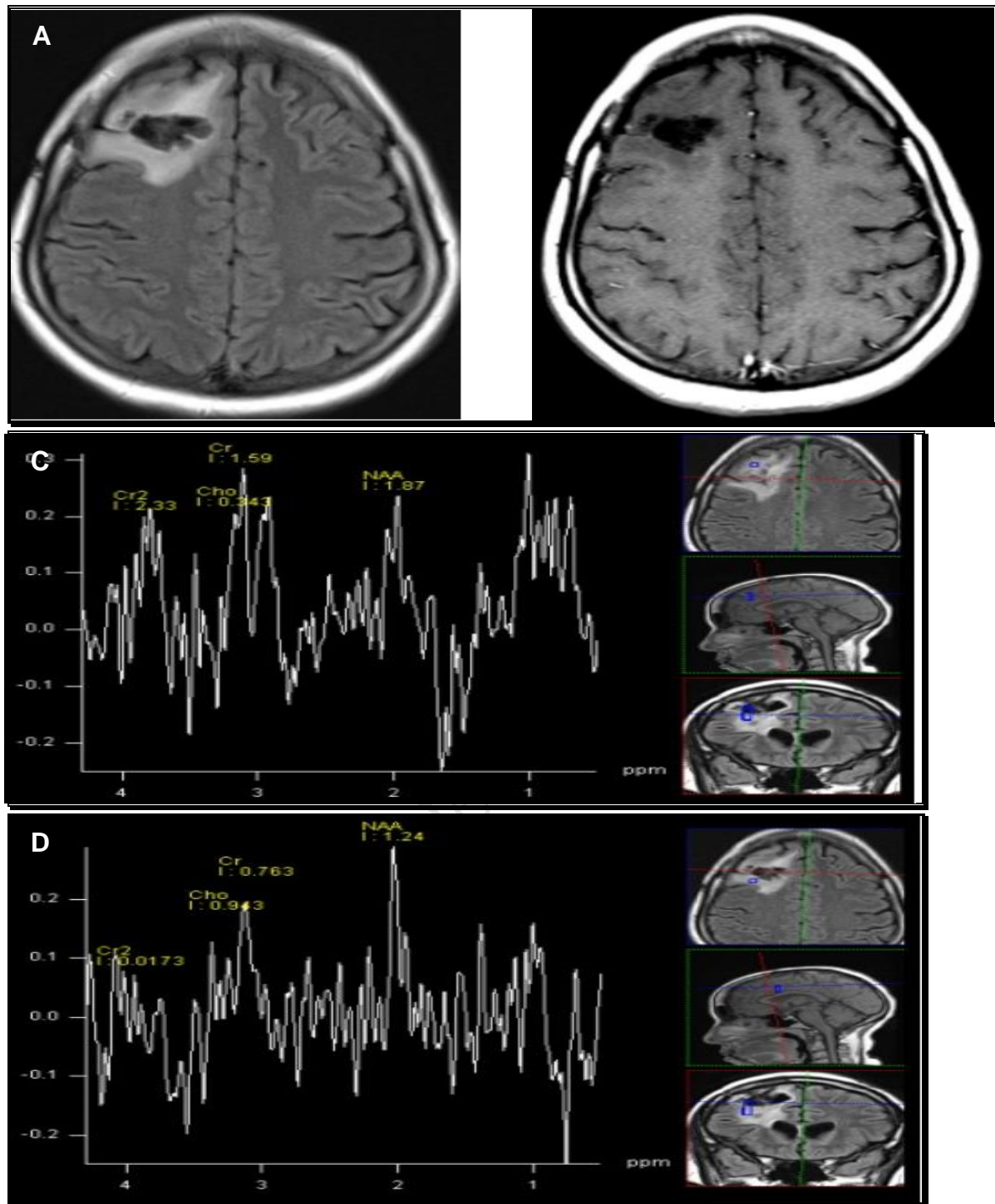


Figure (4): Radiation necrosis. Follow-up MRI and MRS study after resection and chemoradiotherapy for right frontal grade II oligodendroglioma. Axial FLAIR (A) showing right frontal abnormal signal intensity, with perilesional edema. Post-contrast axial T1 weighted image (B) showing no significant enhancement. MRS with short TE with the volume placed over the lesion (C) showing mildly elevated choline peak, slightly reduced NAA and Cr peaks, and prominent Lipid/lactate peak, with slightly elevated Cho/NAA ratio (1.19) and Cho/Cr ratio (1.22). Perilesional voxel with long TE (D) showing no significant elevation of choline peak, indicating no recurrence in the perilesional area.

Table 1: Baseline characteristics, comorbidities and primary pathology of the enrolled cases

			Total (n=30)
Baseline characteristics	Age (years)		39.3± 13.84
	Sex	Male	16 (53.33%)
		Female	14 (46.67%)
	Weight (Kg)		78.2± 10.98
	Height (m)		1.66± 0.04
Comorbidities	BMI (Kg/m²)		28.47± 4.69
	HTN		9 (30%)
	DM		8 (26.67%)
	Glioblastoma		18 (60%)
Primary pathology	Low-grade astrocytoma		4 (13.33%)
	Anaplastic astrocytoma		3 (10%)
	Oligodendroglioma		2 (6.67%)
	CNS Lymphoma		2 (6.67%)
	Medulloblastoma		1 (3.33%)

Data are presented as mean ± SD or frequency (%).HTN: hypertension BMI: body mass index., DM: Diabetes mellitus

Table 2: Radiation dose, interval between completion of radiotherapy to MRS diagnosis, diagnosis and metabolic ratio of the enrolled cases

				Total (n=30)
Radiation dose (Gy)				39.3± 13.84
Interval between completion of radiotherapy to MRS diagnosis (months)				17.33± 8.6
Diagnosis			MRS diagnosis	Histopathologic diagnosis
	Recurrent tumors	23 (76.67%)		24 (80%)
	Radiation necrosis	7 (23.33%)		6 (20%)
Metabolic ratio	NAA / Cho		2.56± 1.11	
	Cr / Cho		2.79± 1.6	

Data are presented as mean ± SD or frequency (%).Cho: choline-containing compounds MRS: Magnetic resonance spectroscopy., NAA: N-acetyl-aspartate

Table 3: The mean interval between completion of radiotherapy to MRS diagnosis and comparison of metabolic ratio based on the MRS diagnosis

	Radiation necrosis (n=7)	Recurrent tumors (n=23)	P value
Mean interval between completion of radiotherapy and MRS diagnosis (months)	12.29± 4.19	18.13± 9.13	0.115
metabolic ratio			
Cho / NAA	1.64± 0.35	2.86± 1.09	0.008*
Cr / Cho	0.64± 0.44	3.16± 1.48	<0.0001*

Data are presented as mean ± SD or frequency NAA: N-acetyl-aspartate, (%). MRS: Magnetic resonance spectroscopy. Cho: choline-containing compounds, *: statically significant p value ≤ 0.05

Table 4: Sensitivity, specificity and diagnostic accuracy of proposed final diagnosis

	Cho/NAA	Cho/Cr	Final diagnosis
Sensitivity	72.00%	85.71%	84.21%
specificity	60.00%	55.56%	75.00%
PPV	90.00%	81.82%	84.21%
NPV	30.00%	62.50%	75.00%
Accuracy	70.00%	76.67%	83.33%

Data are presented as frequency (%). Cho: choline-containing compounds, NAA: N-acetyl-aspartate, PPV: positive predictive value, NPV: negative predictive value.

Cho	Choline
Cho/Cr	choline-to-creatine
CNS	central nervous system
CT	Computed tomography
DM	Diabetes mellitus
DWI	diffusion weighted images
FLAIR	fluid attenuated inversion recovery
FOV	Field-of-view
Gad	gadolinium
Gd-DTPA	gadolinium-diethylenetriamine penta-acetic acid
HTN	hypertension
MR	Magnetic Resonance
MRI	magnetic resonance imaging
MRS	magnetic resonance spectroscopy
NAA	N-acetyl-aspartate
NPV	Negative predictive value
PET	positron emission tomography
ppm	parts per million
PPV	Positive predictive value
RN	Radiation Necrosis
SD	standard deviation
TR	Repetition Time

Discussion

The majority of brain tumors, more than 50%, are intraparenchymal. Although surgery is the primary treatment for these tumors, the neoplastic cells' microscopic dissemination and the tumor's proximity to eloquent regions often impede the complete excision of the tumor. As an adjuvant treatment, radiotherapy is essential for the improved local control of the majority of cases⁽¹⁰⁾. RN is a delayed complication of radiotherapy. Long-term complications that may manifest six months to decades following radiation therapy. In minor arteries, pathologic alterations such as thrombosis, hyalinization, fibrinoid deposition, luminal occlusion, lymphocyte and macrophage infiltration, and endothelial hypertrophy may be observed. Damage to the oligodendroglia is the consequence of vascular endothelial injuries. This means that white matter tissue is often more severely affected than gray matter tissue⁽¹¹⁾.

Regarding the primary pathology, the majority of the studied cases 18 (60%) had glioblastoma, 4 (13.33%) cases had low-grade astrocytoma, 3 (10%) cases had anaplastic astrocytoma, 2 (6.67%) cases had oligodendroglioma, 2 (6.67%) cases had CNS lymphoma and only 1 (3.33%) case had medulloblastoma.

These results are in agreement with Hanif et al.⁽¹²⁾ who stated that Glioblastoma Multiforme are the most commonly occurring tumors of CNS, which account for almost 80% of primary brain tumors.

Also, Schaff and Mellinghoff,⁽¹³⁾ It was determined that glioblastomas account for

approximately 49% of malignant brain tumors, while 30% are diffusely infiltrating lower-grade gliomas.

Further, Ostrom et al.⁽¹⁴⁾ research showed that gliomas made up 26.3% of the cancer population. Although it only makes up 14.2% of tumors overall, glioblastoma is responsible for 50.9% of all malignant tumors in the CNS.

In our research, the interval between completion of radiotherapy to MRS diagnosis ranged from 4 to 32 months with a mean of 17.33 ± 8.6 months.

Anbarloui et al.⁽¹⁵⁾ Both groups had comparable results, as seen by the mean delay between treatment finish and MRS. While the mean interval with RN was 16.3 months, it was 11.1 months with recurring malignancies. Despite the lack of a statistically significant difference ($P = 0.07$), it is worth considering the possibility that RN is an early-stage, uncommon long-term issue, particularly in the six months after radiation therapy.

Regarding the diagnosis of the studied cases, MRS diagnosis showed that recurrent tumors in 23 (76.67%) cases and RN in 7 (23.33%) cases. By histopathologic diagnosis, 24 (80%) cases had recurrent tumors and 6 (20%) cases had RN.

In accordance with our research, Taylor et al.⁽¹⁶⁾ Histological analysis of the case samples confirmed five cases of delayed cerebral necrosis and seven cases of recurrent/residual tumor. Using the MRS criteria, prospective research consistently

identified five individuals with ongoing malignancies and four cases with histologically proven delayed cerebral necrosis.

As well, Anbarloui et al. ⁽¹⁵⁾ and Aseel et al. ⁽¹⁷⁾ MRS is effective in recognizing recurrent brain tumors from necrosis, as concluded.

Based on the results, Cho/NAA and choline-to-creatine (Cho/Cr) were significantly elevated in cases with recurrent tumours compared to those with RN ($P=0.008$, <0.001).

Similarly, Sherif et al. ⁽¹⁸⁾, Eight cases (25%) were diagnosed as post-radiation injury (group II), while twenty-four (75%) were histologically confirmed to have recurrent glioma (group I). The peritumoral infiltration was observed in 18 cases (56.25%) of recurrent glioma. Neoplastic ($n = 24$) lesions exhibited significantly elevated Cho/Cr and Cho/NAA ratios in comparison to non-neoplastic lesions ($n = 8$).

Further, these findings are consistent with Anbarloui et al. ⁽¹⁵⁾ There was a notable disparity ($P < 0.01$) between the mean Cho/NAA titre of 2.72 and 1.46 for recurrent tumors and RN, respectively. In addition, recurring tumors had a clearly larger mean Cho/Cr ratio than RN ($P < 0.01$), with 2.78 for recurrent tumors and 0.6 for RN.

In addition, Aseel et al. ⁽¹⁹⁾ noted that Cho/NAA and Cho/Cr were significantly elevated in cases with recurrent tumours compared to those with RN.

Our results show that MRS diagnosis using Cho/NAA had 72% sensitivity, 60%

specificity, 90% PPV, 30% NPV and 70% diagnostic accuracy. MRS diagnosis using Cho/Cr had 85.71% sensitivity, 55.56% specificity, 81.82% PPV, 62.50% NPV and 76.67% diagnostic accuracy. The proposed final diagnosis had 84.21% sensitivity, 75.00% specificity, 84.21% PPV, 75.00% NPV and 83.33% diagnostic accuracy.

These results are in accordance with Anbarloui et al. ⁽¹⁵⁾ whose findings indicated that the area under the ROC curve for Cho/NAA was 85% and for Cho/Cr was 89%, demonstrating exceptional discrimination between tumor recurrence and RN.

In addition, MRS offers supplementary information regarding the metabolic composition of a specific tissue region by comparing the relative concentrations of multiple metabolites.

Fayed et al. ⁽²⁰⁾ As for the specificity of 83% (95% CI, 36-100%) and sensitivity of 64% (95% CI, 35-87%) for detecting glioma recurrence using a 1.5 threshold of Cho/Cr ratio, those were established.

Furthermore, Traber et al. ⁽²¹⁾ The sensitivity of 72% (95% CI, 53–86%) and specificity of 82% (95% CI, 48–98%) for the differentiation of RN from tumor were demonstrated in a series of 43 cases, as evidenced by an elevated choline peak (50% elevated than contralateral tissue). Not all cases, however, underwent histopathological verification.

Additionally, Chuang et al. ⁽⁴⁾ showed that radiation injury significantly reduced the average relative cerebral blood volume in a contrast-enhancing lesion, whereas tumor recurrence significantly increased it (2.18, 95% CI 0.85-3.50; $p = 0.001$).

Using a fixed-effect model that included all six studies that assessed Cho/Cr ratios, researchers found that tumor recurrence was associated with a significantly elevated pooled difference in means (0.77, 95% CI 0.57-0.98) of the average Cho/Cr ratio than RN ($p = 0.001$). Additionally, recurrent tumor and necrosis showed significantly different Cho to NAA ratios (1.02, 95% CI 0.03-2.00, $p = 0.044$).

Added to that, Travers et al.⁽²²⁾ Out of 25 cases who presented with these types of diagnostic inquiries, 19 underwent MRS and 13 underwent PET CT. The accuracy rate was 81.8%, specificity was 50%, and sensitivity was 100% for MRS.

The limitations of the research where relatively small sample size inevitably lowered the statistical power of the analysis, single-center research making the results less generalizable, short duration of follow-up and MR Perfusion which if used in conjunction with MRS increases the predictive power of same.

Conclusions

Differentiating between tumor recurrence and RN is facilitated by MRS, which is both safe and informative. Various regions of the high-volume lesions must be examined. The meta-analysis demonstrated that the Cho/NAA and Cho/Cr ratios were significantly more accurate predictors of recurrent tumors that had been detected. Thus, MRS imaging serves as an informative instrument for recognizing between necrosis and tumor residual/recurrence.

Therefore, further investigations with larger and stratified sample size for more

accurate results, multi-center research, future studies with longer duration of follow-up and future studies using perfusion MR are recommended

References

1. **Lacy J, Saadati H, James BY.** Complications of brain tumors and their treatment. *Hematol Oncol Clin North Am.* 2012; 26:779-96.
2. **Mayo ZS, Halima A, Broughman JR, Smile TD, Tom MC, Murphy ES, et al.** Radiation necrosis or tumor progression? A review of the radiographic modalities used in the diagnosis of cerebral radiation necrosis. *Neuro Oncol.* 2023; 161:23-31.
3. **Castellano A, Anzalone N.** Radiation and chemotherapy induced injury. *Clinical Neuroradiology* 2019. p. 1-29.
4. **Chuang M-T, Liu Y-S, Tsai Y-S, Chen Y-C, Wang C-K.** Differentiating radiation-induced necrosis from recurrent brain tumor using MR perfusion and spectroscopy: a meta-analysis. *PloS one.* 2016; 11:14-38.
5. **Turnquist C, Harris BT, Harris CC.** Radiation-induced brain injury: current concepts and therapeutic strategies targeting neuroinflammation. *Neurooncol Adv.* 2020; 2:57-70.
6. **Nael K, Bauer AH, Hormigo A, Lemole M, Germano IM, Puig J, et al.** Multiparametric MRI for Differentiation of Radiation Necrosis From Recurrent Tumor in Cases With Treated Glioblastoma. *AJR Am J Roentgenol.* 2018; 210:18-23.
7. **Yang I, Huh NG, Smith ZA, Han SJ, Parsa AT.** Recognizing glioma recurrence from treatment effect after radiochemotherapy and immunotherapy. *Neurosurg Clin N Am.* 2010; 21:181-6.
8. **van Dijken BRJ, van Laar PJ, Holtman GA, van der Hoorn A.** Diagnostic accuracy of magnetic resonance imaging techniques for treatment response evaluation in cases with high-grade glioma, a systematic review and meta-analysis. *Eur Radiol.* 2017; 27:4129-44.
9. **Khanna D, Peltzer C, Kahar P, Parmar MS.** Body Mass Index (BMI): A Screening Tool Analysis. *Cureus.* 2022; 14:22-9.
10. **Lara-Velazquez M, Al-Kharboosh R, Jeanneret S, Vazquez-Ramos C, Mahato D,**

- Tavanaiepour D, et al.** Advances in Brain Tumor Surgery for Glioblastoma in Adults. *Brain Sci.* 2017; 7:20-30.
- 11. Brook I.** Late side effects of radiation treatment for head and neck cancer. *J Radiat Oncol.* 2020; 38:84-95.
- 12. Hanif F, Muzaffar K, Perveen K, Malhi SM, Simjee Sh U.** Glioblastoma Multiforme: A Review of its Epidemiology and Pathogenesis through Clinical Presentation and Treatment. *Asian Pac J Cancer Prev.* 2017; 18:3-9.
- 13. Schaff LR, Mellinghoff IK.** Glioblastoma and Other Primary Brain Malignancies in Adults: A Review. *JAMA.* 2023; 329:574-87.
- 14. Ostrom QT, Price M, Neff C, Cioffi G, Waite KA, Kruchko C, et al.** CBTRUS Statistical Report: Primary Brain and Other Central Nervous System Tumors Diagnosed in the United States in 2016-2020. *Neuro Oncol.* 2023; 25:1-99.
- 15. Anbarloui MR, Ghodsi SM, Khoshnevisan A, Khadivi M, Abdollahzadeh S, Aoude A, et al.** Accuracy of magnetic resonance spectroscopy in distinction between radiation necrosis and recurrence of brain tumors. *Iran J Neurol.* 2015; 14:29-34.
- 16. Taylor JS, Langston JW, Reddick WE, Kingsley PB, Ogg RJ, Pui MH, et al.** Clinical value of proton magnetic resonance spectroscopy for differentiating recurrent or residual brain tumor from delayed cerebral necrosis. *Int J Radiat Oncol Biol Phys.* 1996; 36:51-61.
- 17. Aseel A, McCarthy P, Mohammed A.** Brain magnetic resonance spectroscopy to differentiate recurrent neoplasm from radiation necrosis: A systematic review and meta-analysis. *J Neuroimaging.* 2023; 33:189-99.
- 18. Sherif MF, Salem FM, Almahallawy MA, Abd Algawad AM, Hammad QM.** Role of magnetic resonance spectroscopy in differentiation between recurrence of glioma and post radiation injury. *Egypt J Radiol Nucl Med.* 2014; 45:1233-40.
- 19. Aseel A, McCarthy P, Mohammed A.** Brain magnetic resonance spectroscopy to differentiate recurrent neoplasm from radiation necrosis: A systematic review and meta-analysis. *J Neuroimaging.* 2023; 33:189-99.
- 20. Fayed N, Modrego PJ, Morales H.** Evidence of brain damage after high-altitude climbing by means of magnetic resonance imaging. *Am J Med.* 2006; 119:168-90.
- 21. Träber F, Block W, Flacke S, Lamerichs R, Schüller H, Urbach H, et al.** 1H-MRS of brain tumors in the course of radiation therapy: use of fast spectroscopic imaging and single-voxel spectroscopy for diagnosing recurrence. *RoFo Fortschr Geb Rontgenstr Nuklearned.* 2002; 174:33-42.
- 22. Travers S, Joshi K, Miller DC, Singh A, Nada A, Biedermann G, et al.** Reliability of magnetic resonance spectroscopy and positron emission tomography computed tomography in differentiating metastatic brain tumor recurrence from radiation necrosis. *World Neurosurg.* 2021; 151:1059-68.

to cite this article: Ahmed S. Abd-El-Fattah, Jehan I. Al-Tohamy, Mohammed E. Abd-Elsamea, Hesham E. El-Sheikh, Sherif A. Abd-Elsattar Value of Magnetic Resonance Spectroscopy in Differentiation between Residual/Recurrent Primary Brain Tumors and Radiation Necrosis. *BMFJ XXX*, DOI: 10.21608/bmfj.2025.390118.2443